

1     **Future shift of the relative roles of precipitation and temperature in**  
2             **controlling annual runoff in the conterminous United States**

3

4     Kai Duan<sup>1</sup>, Ge Sun<sup>2</sup>, Steven G. McNulty<sup>2</sup>, Peter V. Caldwell<sup>3</sup>, Erika C. Cohen<sup>2</sup>, Shanlei Sun<sup>4</sup>,  
5     Heather D. Aldridge<sup>5</sup>, Decheng Zhou<sup>4</sup>, Liangxia Zhang<sup>4</sup>, and Yang Zhang<sup>1</sup>

6

7     <sup>1</sup> Department of Marine, Earth, and Atmospheric Sciences, North Carolina State University,  
8     Raleigh, NC, USA

9     <sup>2</sup> Eastern Forest Environmental Threat Assessment Center, USDA Forest Service, Raleigh, NC,  
10    USA

11    <sup>3</sup> Coweeta Hydrologic Laboratory, USDA Forest Service, Otto, NC, USA

12    <sup>4</sup> Key Laboratory of Meteorological Disaster of Ministry of Education, Nanjing University of  
13    Information Science & Technology, Nanjing, Jiangsu, China

14    <sup>5</sup> State Climate Office of North Carolina, North Carolina State University, Raleigh, NC, USA

15

16    Correspondence to:

17    Kai Duan ([kduan@ncsu.edu](mailto:kduan@ncsu.edu)); Ge Sun ([gesun@fs.fed.us](mailto:gesun@fs.fed.us))

18

19

1 **Abstract** This study examines the relative roles of climatic variables in altering annual  
2 runoff in the conterminous United States (CONUS) in the 21<sup>st</sup> century, using a monthly  
3 ecohydrological model (the Water Supply Stress Index model, WaSSI) driven with  
4 historical records and future scenarios constructed from 20 Coupled Model  
5 Intercomparison Project Phase 5 (CMIP5) climate models. The results suggest that  
6 precipitation has been the primary control of runoff variation during the latest decades,  
7 but the role of temperature will outweigh that of precipitation in most regions if future  
8 climate change follows the projections of climate models instead of the historical  
9 tendencies. Besides these two key factors, increasing air humidity is projected to  
10 partially offset the additional evaporative demand caused by warming and consequently  
11 enhance runoff. Overall, the projections from 20 climate models suggest a high degree  
12 of consistency on the increasing trends in temperature, precipitation, and humidity,  
13 which will be the major climatic driving factors accounting for 43 % ~ 50 %, 20 % ~  
14 24 %, and 16 % ~ 23 % of the runoff change, respectively. Spatially, while temperature  
15 rise is recognized as the largest contributor that suppresses runoff in most areas,  
16 precipitation is expected to be the dominant factor driving runoff to increase across the  
17 Pacific Coast and the Southwest. The combined effects of increasing humidity and  
18 precipitation may also surpass the detrimental effects of warming and result in a  
19 hydrologically wetter future in the East. However, severe runoff depletion is more likely  
20 to occur in the central CONUS as temperature effect prevails.

# 1 **1 Introduction**

2 Precipitation and temperature are the two key climatic variables that control land water  
3 balances and thus control water availability for both ecosystem and humans (Lutz et al.,  
4 2014;Milly et al., 2005;Seager et al., 2013;Piao et al., 2010). Changes in temperature  
5 interact with changes in precipitation and cause profound shifts in water balance, such  
6 as snowpack melting and accumulation (Barnett et al., 2005;Zhang et al., 2015),  
7 intensification of hydrologic cycle (Creed et al., 2015;Davis et al., 2015), precipitation  
8 partitioning (Duan et al., 2016b;Zhou et al., 2015), extreme floods and droughts (Duan  
9 et al., 2016a;Trenberth et al., 2014;Duan and Mei, 2014b), and can lead to hydrological  
10 ‘nonstationarity’ (Milly et al., 2008).

11 Surface and subsurface (shallow aquifers) runoff is a critical source of fresh water  
12 for humans (Vörösmarty et al., 2000). The impacts of temperature and precipitation  
13 changes on the magnitude and variability of runoff (Ficklin et al., 2009;Arnell and  
14 Gosling, 2013;Nash and Gleick, 1991;Vano et al., 2012) have drawn particular attention  
15 due to its importance for water supplies. Future changes in precipitation, evaporation,  
16 and plant water use are direct driving forces of runoff generation. Climate change alters  
17 both precipitation and the partitioning of precipitation into evapotranspiration ( $E_T$ ) and  
18 runoff since a warmer climate generally provides more energy for water fluxes between  
19 the land and the atmosphere. Although an increase in precipitation may cause increase  
20 in both  $E_T$  and runoff, the enhanced evaporative demand can result in decreases in  
21 runoff efficiency (ratio of runoff to precipitation) (McCabe and Wolock, 2016). Both  
22 observation and simulation studies in the U.S. suggest that higher  $E_T$  induced by rising

1 temperature is unlikely to be counterbalanced by the increase in precipitation and lead  
2 to less runoff at large scales (Duan et al., 2016b; Jackson et al., 2005; Duan et al., 2017).  
3 Conversely, warming may also cause precipitation decrease in some regions and  
4 exacerbate the effects of temperature on runoff change.

5 Several studies have examined the relative contributions of historical changes in  
6 precipitation and temperature to runoff variation at watershed (Karl and Riebsame,  
7 1989), regional (Ryberg et al., 2014; Gupta et al., 2015), and continental (McCabe and  
8 Wolock, 2011) levels across the conterminous U.S. (CONUS). These studies all agree  
9 that precipitation, instead of temperature, explains most of the long-term change and  
10 variability in runoff during the past century. McCabe and Wolock (2011) suggested that  
11 the effects of temperature on runoff may become more substantial under a warming  
12 climate. However, no study in the literature has rigorously investigated the potential  
13 changes in the roles of precipitation and temperature under future climate scenarios.  
14 According to the Parameter-elevation Relationships on Independent Slopes Model  
15 (PRISM) dataset (<http://prism.oregonstate.edu/>) (Daly et al., 2008), the rate of decadal  
16 change in temperature over the CONUS fluctuated between -0.03 °C and +0.28 °C from  
17 1960s to 2000s. The rate of warming is likely to accelerate under intermediate or high  
18 emission scenarios and increase the pressure of water scarcity in many regions in this  
19 century (IPCC, 2014; Schewe et al., 2014). In addition, future change in climate is  
20 projected to vary spatiotemporally in both direction and magnitude in the CONUS  
21 (Mearns et al., 2012), thus sensitivity of water budget to climate change may be  
22 discrepant across time and space. Although the possible underestimation of the

1 influence of temperature in altering regional water resources has been discussed  
2 recently (Sospedra - Alfonso et al., 2015; Woodhouse et al., 2016), a comprehensive  
3 evaluation under different climate backgrounds and land-cover compositions is still  
4 lacking.

5 We aim to address two questions in this study: (1) to what extent, if any, will the  
6 relative roles of precipitation and temperature in controlling runoff shift, if future  
7 climate changes follow the projections of climate models instead of the tendencies  
8 documented in the recent decades, and (2) how will runoff change in the future and  
9 what are the potential roles of other climatic driving forces besides precipitation and  
10 temperature? In the remainder of the paper, we first describe the methodology of runoff  
11 simulation and sensitivity assessment, and the hydro-climatic datasets used, followed  
12 by the results. Then, the advantages, limitations, and implications of this study are  
13 discussed and the conclusions are drawn.

## 14 **2 Methods**

### 15 **2.1 Study area**

16 The CONUS covers the 48 adjoining states and the District of Columbia. In the  
17 hydrologic unit system developed by the U.S. Geological Survey (USGS)  
18 (<http://water.usgs.gov/GIS/huc.html>), the nation is divided into six levels of hydrologic  
19 units and each unit is identified by a unique hydrologic unit code (HUC) consisting of  
20 two to twelve digits. The first level of classification divides the CONUS into 18 2-digit  
21 HUC areas that are also commonly referred to as Water Resource Regions (WRRs) (Fig.  
22 1). These regions can be further divided into 2,099 8-digit HUC areas, or HUC-8

1 watersheds. This study investigates climate and runoff variations at the resolution of  
2 HUC-8 watershed, as well as the aggregations in each WRR and the entire CONUS.  
3 The full lists and boundaries of hydrologic units at different levels can be found in the  
4 Watershed Boundary Dataset (<https://datagateway.nrcs.usda.gov/>).

## 5 **2.2 Runoff modeling**

6 The runoff responses to climate change and variability were modeled with the Water  
7 Supply Stress Index model (WaSSI). WaSSI is a monthly ecohydrological model that  
8 was developed to capture land-cover specific large-scale water balance in the  
9 conterminous US based on empirical and physically based parameters (Caldwell et al.,  
10 2012;Sun et al., 2011b). It was integrated from a snow model, a  $E_T$  model, and a soil  
11 moisture accounting model. A conceptual snow sub-model (McCabe and Markstrom,  
12 2007) is used to partition the total precipitation into rainfall and snowfall, and to  
13 estimate snowpack melt/accumulation and snow water equivalent with concern of the  
14 mean elevation, latitude, and air temperature in the watershed.  $E_T$  is calculated with an  
15 ecosystem  $E_T$  model developed from the empirical relationships between  $E_T$  and  
16 precipitation, potential evapotranspiration (PET), and leaf area index (LAI) (Sun et al.,  
17 2011a;Sun et al., 2011b). These  $E_T$  functions were established for 10 different land-  
18 cover classes independently to account for the different water demand within different  
19 vegetation, ranging from cropland, deciduous forest, evergreen forest, mixed forest,  
20 grassland, shrubland, wetland, open water, urban area, to barren land. Then, this  $E_T$   
21 estimation is further constrained by soil water availability, which is simulated using the  
22 algorithms of Sacramento Soil Moisture Accounting model (SAC-SMA) (Burnash,

1 1995), as well as the processes of infiltration and runoff generation at monthly basis.  
2 SAC-SMA is a classic rainfall-runoff conceptual model that has been successfully used  
3 by the U.S. National Weather Service (NWS) to issue river forecasts across the country  
4 for decades. Necessary inputs for WaSSI include monthly precipitation, air temperature,  
5 PET, LAI, and land-cover composition. In this study, the spatial distribution of LAI and  
6 the 10 land-cover classes were assumed to be static over time. Monthly climate data  
7 were first scaled to watersheds by the area-weighted averages. All the water balance  
8 components were calculated independently for each land cover class within each  
9 watershed, and then were aggregated monthly means. The model parameters were  
10 acquired from several previous studies, including: (1) The parameters of snow sub-  
11 model (4 parameters for each WRR) were estimated for each WRR by comparing  
12 regional monthly mean snow water equivalent to remotely sensed values from the Snow  
13 Data Assimilation System (McCabe and Markstrom, 2007;Caldwell et al., 2012). (2)  
14 The parameters of  $E_T$  sub-model (3 empirical parameters for each land-cover type) were  
15 estimated by empirical relationships derived from eddy covariance or sapflow  
16 measurements at multiple sites (Sun et al., 2011a;Sun et al., 2011b). (3) SAC-SMA  
17 parameters (11 parameters for each watershed) used to drive the soil water balance sub-  
18 model were developed from soil physical characteristics documented by the State Soil  
19 Geographic Database (<http://soildatamart.nrcs.usda.gov>) (Anderson et al., 2006;Koren  
20 et al., 2003).

21 The WaSSI model has been validated against observations at USGS gauged sites at  
22 the levels of both 8-digit (Caldwell et al., 2012) and 12-digit HUC watersheds (Sun et

1 al., 2015b). We here verify the model performance at CONUS and WRR scales to  
 2 complement to previous validations. The simulated annual runoff, driven by monthly  
 3 precipitation and temperature from the PRISM dataset, was compared against the  
 4 USGS measurements over the entire CONUS (Fig. 2a&2c) and in the 18 WRRs (Fig.  
 5 2b&2d) for the time period of 1961-2010. Despite a slight overestimation of the  
 6 minimums, WaSSI shows reliable accuracy in capturing annual runoff at both CONUS  
 7 and WRR scales, with R-square statistic reaching 0.91 and 0.95, and Root Mean  
 8 Squared Error (RMSE) limited to 29 and 55 mm yr<sup>-1</sup>, respectively.

### 9 **2.3 Quantifying the independent effects of climatic variables**

10 Large-scale water balance can be described as runoff ( $R$ ) equals precipitation ( $P$ ) minus  
 11  $E_T$  and changes in soil moisture ( $S_M$ ) and the hydrologically connected snowpack ( $S_P$ ):

$$12 \quad R = P - E_T + dS_M/dt + dS_P/dt \quad (1)$$

13 While  $P$  is the primary water input, changing temperature ( $T$ ) and other climatic factors  
 14 interact with each other and affects  $R$  by altering the melt/accumulation of snowpack  
 15 and controlling  $E_T$  with the constraints of vegetation and soil moisture.

16 Here we developed a simple approach of sensitivity test to examine the relative roles  
 17 of climatic variables in  $R$  variation, as:

$$18 \quad \Delta R = \sum_{i=1}^N E_{Ci} + E_{Int} \quad (2)$$

19 where  $\Delta R$  denotes the change in  $R$ , which equals the combined effect of variations in  
 20 all the climatic variables ( $C_i, i=1,2,\dots,N$ ).  $\Delta R$  can be decomposed into the independent  
 21 effects of each variable ( $E_{Ci}$ ) and the effect of interactions among them ( $E_{Int}$ ). From a  
 22 pre-change period ( $t_1$ ) to a post-change period ( $t_2$ ),  $\Delta R$  is quantified by  $R$  change (%)  
 23 driven by changes in all the variables, as the difference between



1  $R(CI_{t2}, \dots, Ci_{t2}, \dots, CN_{t2})$  and  $R(CI_{t1}, \dots, Ci_{t1}, \dots, CN_{t1})$ ; while  $E_{Ci}$  is estimated by  
 2  $R$  change driven by changes in the variable  $Ci$  only, as the difference between  
 3  $R(CI_{t1}, \dots, Ci_{t2}, \dots, CN_{t1})$  and  $R(CI_{t1}, \dots, Ci_{t1}, \dots, CN_{t1})$ .  $E_{Int}$  is calculated as the  
 4  $\Delta R$  minus  $\sum_{i=1}^N E_{Ci}$ , representing the changes in  $R$  that cannot be accounted for by the  
 5 independent effects. Given that the changing climatic variables may cause either  
 6 positive or negative effects on  $R$ , their contributions (%) are quantified by the relative  
 7 weights, as

$$8 \quad C(Ci) = 100 \times |E_{Ci}| / (\sum_{i=1}^N |E_{Ci}| + |E_{Int}|) \quad (3)$$

## 9 **2.4 Modeling experiments**

### 10 **2.4.1 Climate projection**

11 Climate data downscaled from the raw outputs of 20 Global Climate Models (GCMs)  
 12 (Table 1) of the fifth phase of the Coupled Model Inter-comparison Project (CMIP5)  
 13 (the MACAv2-LIVNEH dataset, Livneh et al., 2013, available at  
 14 <http://maca.northwestknowledge.net/>) were used to test the potential future changes in  
 15  $R$ . This dataset includes the CMIP5 experiments of ‘historical’, Representative  
 16 Concentration Pathways (RCP) 4.5, and RCP8.5, which correspond to the climate  
 17 forcings (i.e., greenhouse gases emissions, aerosols, land use feedbacks, etc.) observed  
 18 in the history and projected in a future with the radiative forcing reaching 4.5 and 8.5  
 19  $W m^{-2}$  in 2100 (equivalent to 650 ppm and 1370 ppm  $CO_2$ ), respectively (Moss et al.,  
 20 2010; IPCC, 2014). The used climatic variables include monthly  $P$ , maximum and  
 21 minimum  $T$ , solar radiation ( $Rs$ ), wind speed ( $Ws$ ), and specific humidity ( $Sh$ ) spanning  
 22 from 1950 to 2099 (Fig. 3).

1 To evaluate the  $R$  responses to various changes in future climates, we conducted four  
2 30-year simulation experiments: (i) RCP4.5/2030s (S1 scenario) — near future 2020-  
3 2049 under RCP4.5; (ii) RCP4.5/2080s (S2) — far future 2070-2099 under RCP4.5;  
4 (iii) RCP8.5/2030s (S3) — near future 2020-2049 under RCP8.5; (iv) RCP8.5/2080s  
5 (S4) — far future 2070-2099 under RCP8.5. These four future scenarios cover two post-  
6 change time periods (2030s and 2080s) and are compared to the historical condition in  
7 1970-1999 (1980s) that represents the baseline level. Traditional sensitivity test  
8 methods usually assume a fixed amount of change (Karl and Riebsame, 1989) or allow  
9 one (or more) of the variables to remain constant over time (McCabe and Wolock, 2011).  
10 In this study, the 30-year-long continuous climate series were used to examine the long-  
11 term patterns while implicitly incorporating the inter- and intra-annual variations. This  
12 large set of climate projections was collected to enable a robust quantification of the  
13 major uncertainties from GCM structure and emission scenario.

#### 14 **2.4.2 Estimation of potential evapotranspiration**

15 Hamon's PET equation has been used for PET estimation in previous WaSSI  
16 simulations because it only requires mean temperature as input and has shown reliable  
17 correlation with actual  $E_T$  in historical periods (Lu et al., 2005; Vörösmarty et al., 1998).  
18 Essentially, temperature-based methods perform well because  $T$  is correlated with  
19 radiation and humidity at monthly timescale (Sheffield et al., 2012). Such correlations  
20 are the physical bases of the empirical  $E_T$  functions, through which variability in  $P$ ,  $T$ ,  
21 and LAI was able to explain the main controls of evaporation and transpiration fluxes  
22 without including the radiative and aerodynamic variables. However, recent studies

1 revealed that the bias in temperature-based methods could be amplified in future  
2 scenarios of global warming, leading to overestimation of PET and ultimately  $E_T$  and  
3 the severity of land surface drying (Milly and Dunne, 2011; Sheffield et al., 2012).  
4 Penman-Monteith (PM) reference  $E_T$  (Allen et al., 1998), as a commonly used  
5 alternative PET model, incorporates the effects of surface temperature, humidity, wind,  
6 and radiation, and is considered the most reliable PET approach where sufficient  
7 meteorological data exist (Kingston et al., 2009; Feng and Fu, 2013).

8 In this case, using Hamon equation would lead to  $130 \text{ mm yr}^{-1}$  larger PET increase  
9 from the baseline to RCP8.5/2080s than that using PM equation (Fig. 4). We assume  
10 that the PM PET projections are more reasonable because the effects of future changes  
11 in  $R_s$ ,  $W_s$ , and  $Sh$  are included as well as  $T$ . In the remaining of this paper, we will focus  
12 on analyzing the  $R$  changes and the independent effects of five climatic variables based  
13 on PM PET, i.e.,  $P$ ,  $T$  (including changes in maximum  $T$ , minimum  $T$ , and mean  $T$  that  
14 was estimated as the average of maximum and minimum),  $R_s$ ,  $W_s$ , and  $Sh$ . Effects of  $P$   
15 and  $T$  evaluated from simulations of Hamon PET will also be investigated to address  
16 the consistency and discrepancy caused by using different PET methods.

### 17 **3. Results**

#### 18 **3.1 Projected changes in runoff**

19 Changes in mean annual  $R$  under future climate change scenarios vary among HUC-8  
20 watersheds (Fig. 5) and WRRs (Fig. 6) across the CONUS. Runoff depletion is  
21 projected to cover most part of the central CONUS across WRR7~WRR12, with largest  
22 decreases over 50 % found in the south of WRR10 (Missouri) under RCP8.5. Increases

1 are mainly projected in the Southwest, the north of Missouri, and regions along the  
2 Atlantic Coast and Pacific Coast. Extreme increases over 100 % are projected in several  
3 arid watersheds in WRR15 (Lower Colorado) and WRR16 (Great Basin). However, this  
4 may be caused by the inability of GCMs in reproducing the low  $P$  values in these  
5 extremely dry areas. Although the general spatial patterns appear to be similar in the  
6 four scenarios, there is an evident expansion of the areas showing either extreme  
7 increasing or decreasing trend from 2030s to 2080s under both RCP4.5 (Fig. 5a-5b) and  
8 RCP8.5 (Fig. 5c-5d) scenarios.

9 The large variability of regional changes in  $R$  (Fig. 6) indicates considerable  
10 uncertainties from GCM structure. In most cases, the uncertainty range is limited to  
11  $-30\% \sim +30\%$ , showing both positive and negative changing signals. The distributions  
12 of the median lines and Inter-Quartile Ranges (IQRs) suggest a hydrologically drier  
13 future in WRR7~12 and WRR14 (Upper Colorado), where consistent decreasing signal  
14 is found in all the scenarios. Increasing trend can be found in WRR1 (New England),  
15 WRR2 (Mid-Atlantic), WRR17 (Pacific Northwest), and WRR18 (California).  
16 Generally, the uncertainty ranges tend to increase from 2030s to 2080s under both RCPs,  
17 and reach a particularly high level under RCP8.5/2080s. There is a noticeable  
18 consistency in the pattern that the GCMs agree more on the simulations in 2030s while  
19 the uncertainty aggregates over time toward 2080s, which implies the limitation of the  
20 state-of-the-art GCMs in predicting farther future.

### 21 **3.2 Independent effects of climate variables**

22 The changes in  $R$  discussed above are under the combined impact of changing  $P$ ,  $T$ ,  $R_s$ ,

1 *Ws*, and *Sh*. The independent effects of these factors over the entire CONUS are  
2 illustrated in Fig.7a-7b. *P* and *T* are clearly the two most influential factors, which are  
3 projected to cause divergent changes in *R* due to the increase in *P* (+15 ~ +31 mm yr<sup>-1</sup>)  
4 and *T* (+1.8 ~ +5.3 °C). The median values show that annual *R* under the independent  
5 *P* effect is expected to increase by 13 mm yr<sup>-1</sup> (4 %) in 2030s and 24 mm yr<sup>-1</sup> (8 %) in  
6 2080s under RCP4.5, and by 21 (7 %) and 30 (10 %) mm yr<sup>-1</sup> at the same time under  
7 RCP8.5. In contrast, the independent effects of *T* reach -32 (-11 %), -50 (-17 %), -34 (-  
8 12 %), and -80 (-28 %) mm yr<sup>-1</sup> in the scenarios S1~S4. The negative effect of rising *T*  
9 is expected to exceed the positive effect of increasing *P* and lead to overall decrease in  
10 *R*. However, *Sh*, the third largest contributor, will enhance *R* by 3 % ~ 12 % and largely  
11 offset the *T* effects. Significant increasing trend in *Sh* is projected under both RCP4.5  
12 and RCP8.5 (Fig. 3e), which will suppress vapor pressure deficit and thus partially  
13 counterbalance the increasing evaporative demand caused by warming. Meanwhile, the  
14 effects of *Rs* (slightly negative), *Ws* (slightly positive), and interactions among the  
15 factors (*Int*) are relatively minimal (< 3 %), suggesting that the variations in *T*, *P*, and  
16 *Sh* can explain the major changes in *R*.

17 It is worth noticing that much larger uncertainty ranges can be found in the *P* effects.  
18 Compared to the highly consistent increases in *T* and *Sh*, the 20 GCMs constantly  
19 disagree on the changing direction of *P*. Under RCP8.5/2080s, the multi-model result  
20 of *P* effect ranges from -11 % to 24 %, and the IQR also reaches the highest level (13 %).  
21 It indicates that uncertainty in *P* projection is still the largest contributor to the  
22 uncertainty in *R* simulations, especially in the far future.

1 We also compared these results with those evaluated based on Hamon PET (Fig. 7c),  
2 and found some similar features. The differences in independent effects of  $P$  and  $T$   
3 between the two sets of results are mostly smaller than 5 %, and both results show that  
4  $T$  effect would be twice as large as  $P$  effect at CONUS scale. This suggest that the bias  
5 in PET model structure is not likely to turn over the relative importance of  $P$  and  $T$   
6 effects as long as  $E_T$  model is properly calibrated. However, the projected decreases in  
7  $R$  (i.e., the ‘Total’ effects) are obviously more severe when using Hamon PET because  
8 the positive effect of increasing humidity is not considered.

### 9 **3.3 Relative contributions of precipitation and temperature**

10 Table 2 summarizes the relative contributions of  $P$  and  $T$  to  $R$  change for the historical  
11 and future periods in 18 WRRs and the entire CONUS. Historical changes in  $P$ ,  $T$ , and  
12 their effects on  $R$  were tested using PRISM climate data spanning from January 1960  
13 to December 2010. Given the significant spatial and temporal variability in  $R$  trend  
14 across the CONUS (Mauget, 2003;McCabe and Wolock, 2002, 2011;Gupta et al., 2015),  
15 a consistent breakpoint is statistically unavailable. We hereby took 1985 as the  
16 breakpoint year for all the watersheds and evaluated the multi-decadal mean changes  
17 from 1961-1985 (pre-change period) to 1986-2010 (post-change period). Although the  
18 selection of different breakpoints may cause certain deviations, the analysis can provide  
19 a comparable benchmark for exploring the shifts in future scenarios at a multi-decadal  
20 scale. Unsurprisingly, the results of these latest decades show the prevailing role of  $P$   
21 in nearly all the regions, with WRR14 being the only exception. In the future periods  
22 (from baseline to S1~S4), however, results derived from both PM and Hamon PET

1 suggest that the role of  $T$  rise will surpass  $P$  and become the largest driver in most of  
2 the regions (15~16 out of 18 WRRs) in the future. In contrast, a larger mean  
3 contribution of  $P$  can be occasionally found in the Atlantic Coast (WRR1,2), Pacific  
4 Coast (WRR18), and the Southwest (WRR12,15). Considering that the inconsistency  
5 among GCMs may make the recognition of larger contributor dubious, we used  
6 Wilcoxon signed-rank test (Gibbons and Chakraborti, 2011) to assess the statistical  
7 significance of the difference between each pair of  $P$  and  $T$  contributions (i.e., 20  
8 samples from the 20 GCMs). The test results reveal high agreement among GCMs on  
9 the prominent role of  $T$  across most regions (underlined in Table 2).

10 At CONUS level, the mean contributions of  $P$  and  $T$  are projected to lie within 20 %  
11 ~ 24 % and 43 % ~ 50 % using PM PET, and 33%~40% and 55 % ~ 62 % using Hamon  
12 PET, suggesting a similar shift in the relative importance of these two key driving  
13 factors. However, future changes in  $Sh$ ,  $Rs$ , and  $Ws$  account for another 16 % ~ 23 %,   
14 2 % ~ 7 %, and 1 % ~ 4 % of  $R$  change respectively, and indirectly affect the attributions  
15 to  $P$  and  $T$ . For example, the  $R$  increase in WRR1 would be completely attributed to  $P$   
16 increase if  $Sh$  was not considered, and thus lead to an overestimation of  $P$  contribution.

### 17 **3.4 Spatial distribution of the major driving factors**

18 To further investigate the spatial pattern of future climatic controls on annual  $R$ , we  
19 mapped the coverage of dominant driving factors (Fig. 8) and examined its consistency  
20 with the changing trend in  $R$  at watershed scale (Table 3). Judging by multi-model  
21 ensemble means,  $P$  and  $T$  are the largest driving factor in 10 % ~ 22 % and 68 % ~ 89 %  
22 of the CONUS area. High consistency on their dominant roles (80 % or more of the 20

1 GCMs agree on the sign) can be found in 4 % ~ 7 % and 21 % ~ 41 % of the CONUS,  
2 respectively. As  $P$  and  $T$  are projected to keep increasing, the coverages of  $P$ -dominant  
3 and  $T$ -dominant areas are also expected to expand from 2030s to 2080s. A directional  
4 change suggests that rising  $T$  will become more influential in the east (WRR1~6), while  
5  $P$  will prevail in more watersheds across the west (WRR13~18). Although the  
6 aggregated effect of  $Sh$  is quite close to that of  $P$  at large scales, it is only expected to  
7 play a dominant role in several watersheds (1 % in area) across the borders between  
8 WRR10 and WRR11 under RCP8.5/2080s.

9 The  $P$ -dominant areas that mainly distributed in the Southwest (WRR13,15) and  
10 Pacific Coast (WRR17,18) show clear signals of increasing  $R$ , driven by the widespread  
11 increase in  $P$ . On the other hand, only two thirds of the  $T$ -dominant areas coincide with  
12 the areas of decreasing  $R$ , covering a large part of the central CONUS (WRR7,9,10,11)  
13 and a number of watersheds scattered in the Northwest (WRR14,16,17). Although  $T$  is  
14 also identified as the most influential factor in the eastern regions WRR1~5, the  
15 combined effect of other four factors, primarily  $P$  and  $Sh$ , is projected to exceed the  $T$   
16 effect and lead to an increase in  $R$ .

## 17 **4. Discussion**

### 18 **4.1 Spatial patterns of future runoff change**

19 This study characterizes and generalizes large-scale relationships among changing  $P$ ,  $T$ ,  
20 and  $R$  despite the large geographic differences. The coherence in the spatial dynamics  
21 of  $R$  trend and the corresponding climatic drivers shows a rough pattern:  $T$  change  
22 dominates  $R$  decrease while  $P$  and  $Sh$  changes dominate  $R$  increase. However, it should



1 be interpreted with limitations on time scale and underlying surface features. This  
2 pattern does not hold true in all the watersheds due to the nonlinear complexity of  $R$   
3 response to climate change at various time scales, as well as the influence of other  
4 watershed characteristics (e.g., topography, land-use, soil property). For example, slight  
5 decreases in annual  $P$  but somewhat increases in annual  $R$  are projected in south Texas  
6 due to the changes in intra-annual climate variability. The role of  $T$  may also become  
7 more positive in regions where water availability is dominated by snow melting  
8 (Barnett et al., 2005;Lutz et al., 2014). Besides, local  $R$  can be affected by other factors,  
9 such as land-cover evolution and the direct effects of atmospheric composition on  
10 transpiration (Gedney et al., 2006;Zhang et al., 2001;Zhang et al., 2015).

#### 11 **4.2 The role of land cover and land use**

12 Land cover, LAI, and soil are important controls on catchment water balance and  $R$   
13 sensitivity to climate change (Zhang et al., 2001;Bosch and Hewlett, 1982;Cheng et al.,  
14 2014). This study specifically focused on evaluating the separate and combined effects  
15 of changing climates on  $R$  within a static land cover/land use. We did not consider the  
16 potential evolution of land cover and its interactions with water balance. We made no  
17 explicit tabulation of the impact of land cover/land use on the  $R$  responses to climate  
18 change, but we did incorporate it as a key factor by estimating  $E_T$  with a set of functions  
19 of climate, LAI, and soil moisture capacity and deficit. Across the land cover classes,  
20 the uncertainty ranges of independent contributions of  $P$  (13 % ~ 30 %) and  $T$  (39 % ~  
21 51 %) are relatively small compared to the ranges across WRRs (18 % ~ 47 % and 29 %  
22 ~ 52 %). This may be because the discrepancy across different land covers is largely

1 offset by the different climate backgrounds across the country. Evaluation of future land  
2 cover change and its impact on  $R$  is out of the scope of this study. However, our results  
3 imply that the potential impact of land cover change might not be large enough to alter  
4 the relative significance of  $P$  and  $T$  in controlling future continental water availability.

### 5 **4.3 Implications for water and land management**

6 Our results have important implications for water and land management across the  
7 CONUS. Water resources planning may need to prepare different management  
8 strategies for areas facing contrasting future hydrological conditions. Additional water  
9 storage such as reservoirs may be needed in regions expecting more  $R$ , while inter-basin  
10 water transfer, improving water use efficiency, and other water conservation measures  
11 such as rain harvesting, and waste water recycling should be implemented for areas  
12 expecting water shortages. The vast croplands across central U.S. are likely to be  
13 threatened by rising  $T$  and diminishing water availability for irrigation and food  
14 production. Adaptations in cropping systems and irrigation strategy are needed to  
15 secure food supply and increase resiliency to drought and changing climate (Challinor  
16 et al., 2014;Teixeira et al., 2013). The drier and hotter conditions may also result in  
17 increasing water stress, higher risks of tree insects and disease outbreaks, and  
18 catastrophic wildfires in forests (Dale et al., 2001) (e.g., National Forests in WRR14,  
19 16, 17) and grasslands (e.g., in WRR10~11). Innovative land management practices  
20 such as forest thinning and fuel management, irrigation, and planting drought-tolerant  
21 species are vital to minimize the potential risk and vulnerability to climate change and  
22 reduce the threats to ecosystems and society (Sun et al., 2015a;Grant et al., 2013;Vose

1 et al., 2016).

## 2 **4.4 Uncertainties and caveats**

3 Considerable uncertainty lies in the projection of future climate changes from the 20  
4 GCMs. The uncertainty ranges under both RCP4.5 and RCP8.5 show significant  
5 expansions over time from 2030s to 2080s. In particular, the large uncertainty in  
6 predicting future  $P$  may substantially compromise the reliability in evaluating either  $R$   
7 change or the roles of  $P$  and  $T$  (Karl and Riebsame, 1989;Piao et al., 2010). Although  
8 the results allow us to draw some conclusions on the general patterns, uncertainties are  
9 large and vary differently across space and time. There are certain limitations in this  
10 evaluation that should be noted when interpreting the results. First, we did not  
11 incorporate other sources of uncertainty, such as the methodology of downscaling  
12 (Duan and Mei, 2014a;Chen et al., 2011), and structure and parameters of hydrologic  
13 model (Jung et al., 2012). Although the selections of GCM and emission scenario are  
14 more likely to be the largest sources of uncertainty in hydro-climatic modeling (Kay et  
15 al., 2009;Wilby and Harris, 2006;Duan and Mei, 2014b), the other sources may also  
16 affect the results to different extents. The roles of uncertainties from different sources  
17 can be particularly equivocal when investigating seasonal/monthly variability and  
18 extreme events (Bosshard et al., 2013;Giuntoli et al., 2015;Bae et al., 2011;Kay et al.,  
19 2009). Second, we focused on the independent effects of potential climate changes,  
20 while assuming the inter-relationship among the meteorological variables and water-  
21 balance components remains the same as in historical periods. In future studies,  
22 improved climate datasets and better representation of the physical mechanisms of

1 climatic factors (e.g., radiation, Bohn et al., 2013; wind speed, McVicar et al., 2012)  
2 are needed to reduce uncertainties.

### 3 **5. Conclusions**

4 This study evaluates the relative roles of precipitation and air temperature, as well as  
5 solar radiation, wind speed, and air humidity, in altering annual runoff across the  
6 CONUS based on a large ensemble of simulations using data from both historical  
7 measurements and CMIP5 GCMs projections. Despite the large uncertainty and spatial  
8 variability involved in the results, two robust conclusions can be drawn at the CONUS  
9 and regional scales on multi-decadal basis. First, the role of temperature will outweigh  
10 that of precipitation in a continued warming future in the 21<sup>st</sup> century, in spite that  
11 precipitation has been the primary control of runoff variation during the latest decades.  
12 The projections from 20 climate models suggest a high degree of consistency on the  
13 increasing trends in both precipitation and temperature, but the negative effect of  
14 temperature is expected to exceed the positive effect of precipitation on runoff change  
15 in most regions. Over the entire CONUS, temperature is projected to be the largest  
16 contributor (43 % ~ 50 %), followed by precipitation (20 % ~ 24 %), humidity  
17 (16%~23%), solar radiation (2 % ~ 7 %), and wind speed (1 % ~ 4 %). Spatially,  
18 precipitation is likely to be the dominant driving factor for runoff increase across the  
19 Pacific Coast and the Southwest, while temperature will be more influential in the  
20 central CONUS and parts of the Northwest and cause runoff decreases.

21 Second, increasing humidity is expected to partially offset the additional evaporative  
22 demand caused by warming, and consequently enhance runoff wide across the country.

1 Although the rising temperature is projected to be the largest control of runoff change  
2 in the eastern CONUS, the combined effects of increasing humidity and precipitation  
3 will surpass the detrimental effects of warming and result in a hydrologically wetter  
4 future. This study also raises concern on the choice of PET method. It has been well  
5 acknowledged in hydrometeorological communities that temperature-based PET  
6 methods tend to be oversensitive to temperature change. Our results further demonstrate  
7 that the main risk of using temperature-based PET is overlooking the effects of other  
8 changing climatic variables (mainly humidity in this case), which have not been as  
9 widely measured as temperature and are relatively understudied, rather than  
10 overestimating the effects of temperature.

## 1 **References**

- 2 Allen, R. G., Pereira, L. S., Raes, D., and Smith, M.: Crop evapotranspiration-Guidelines for computing  
3 crop water requirements-FAO Irrigation and drainage paper 56, FAO, Rome, 300, D05109, 1998.
- 4 Anderson, R. M., Koren, V. I., and Reed, S. M.: Using SSURGO data to improve Sacramento Model a priori  
5 parameter estimates, *Journal of Hydrology*, 320, 103-116, 2006.
- 6 Arnell, N. W., and Gosling, S. N.: The impacts of climate change on river flow regimes at the global scale,  
7 *Journal of Hydrology*, 486, 351-364, 2013.
- 8 Bae, D.-H., Jung, I.-W., and Lettenmaier, D. P.: Hydrologic uncertainties in climate change from IPCC AR4  
9 GCM simulations of the Chungju Basin, Korea, *Journal of Hydrology*, 401, 90-105, 2011.
- 10 Barnett, T. P., Adam, J. C., and Lettenmaier, D. P.: Potential impacts of a warming climate on water  
11 availability in snow-dominated regions, *Nature*, 438, 303-309, 2005.
- 12 Bohn, T. J., Livneh, B., Oyster, J. W., Running, S. W., Nijssen, B., and Lettenmaier, D. P.: Global evaluation  
13 of MTCLIM and related algorithms for forcing of ecological and hydrological models, *Agricultural and  
14 forest meteorology*, 176, 38-49, 2013.
- 15 Bosch, J. M., and Hewlett, J.: A review of catchment experiments to determine the effect of vegetation  
16 changes on water yield and evapotranspiration, *Journal of hydrology*, 55, 3-23, 1982.
- 17 Bosshard, T., Carambia, M., Goergen, K., Kotlarski, S., Krahe, P., Zappa, M., and Schär, C.: Quantifying  
18 uncertainty sources in an ensemble of hydrological climate - impact projections, *Water Resources  
19 Research*, 49, 1523-1536, 2013.
- 20 Burnash, R.: The NWS river forecast system-catchment modeling, in: *Computer models of watershed  
21 hydrology.*, edited by: Singh, V., Water Resources Publications, Littleton, Colorado, 311-366, 1995.
- 22 Caldwell, P., Sun, G., McNulty, S., Cohen, E., and Moore Myers, J.: Impacts of impervious cover, water  
23 withdrawals, and climate change on river flows in the conterminous US, *Hydrology and Earth System  
24 Sciences*, 16, 2839-2857, 2012.
- 25 Challinor, A., Watson, J., Lobell, D., Howden, S., Smith, D., and Chhetri, N.: A meta-analysis of crop yield  
26 under climate change and adaptation, *Nature Climate Change*, 4, 287-291, 2014.
- 27 Chen, J., Brissette, F. P., and Leconte, R.: Uncertainty of downscaling method in quantifying the impact  
28 of climate change on hydrology, *Journal of Hydrology*, 401, 190-202, 2011.
- 29 Cheng, L., Zhang, L., Wang, Y.-P., Yu, Q., Eamus, D., and O'Grady, A.: Impacts of elevated CO<sub>2</sub>, climate  
30 change and their interactions on water budgets in four different catchments in Australia, *Journal of  
31 Hydrology*, 519, 1350-1361, 2014.
- 32 Creed, I., Hwang, T., Lutz, B., and Way, D.: Climate warming causes intensification of the hydrological  
33 cycle, resulting in changes to the vernal and autumnal windows in a northern temperate forest,  
34 *Hydrological Processes*, 29, 3519-3534, 2015.
- 35 Dale, V. H., Joyce, L. A., McNulty, S., Neilson, R. P., Ayres, M. P., Flannigan, M. D., Hanson, P. J., Irland, L.  
36 C., Lugo, A. E., and Peterson, C. J.: Climate Change and Forest Disturbances Climate change can affect  
37 forests by altering the frequency, intensity, duration, and timing of fire, drought, introduced species,  
38 insect and pathogen outbreaks, hurricanes, windstorms, ice storms, or landslides, *BioScience*, 51, 723-  
39 734, 2001.
- 40 Daly, C., Halbleib, M., Smith, J. I., Gibson, W. P., Doggett, M. K., Taylor, G. H., Curtis, J., and Pasteris, P. P.:  
41 Physiographically sensitive mapping of climatological temperature and precipitation across the  
42 conterminous United States, *International Journal of Climatology*, 28, 2031-2064, 2008.
- 43 Davis, J., O'Grady, A. P., Dale, A., Arthington, A. H., Gell, P. A., Driver, P. D., Bond, N., Casanova, M.,

1 Finlayson, M., and Watts, R. J.: When trends intersect: The challenge of protecting freshwater  
2 ecosystems under multiple land use and hydrological intensification scenarios, *Science of The Total*  
3 *Environment*, 534, 65-78, 2015.

4 Duan, K., and Mei, Y.: A comparison study of three statistical downscaling methods and their model-  
5 averaging ensemble for precipitation downscaling in China, *Theoretical and applied climatology*, 116,  
6 707-719, 2014a.

7 Duan, K., and Mei, Y.: Comparison of Meteorological, Hydrological and Agricultural Drought Responses  
8 to Climate Change and Uncertainty Assessment, *Water Resources Management*, 28, 5039-5054, 2014b.

9 Duan, K., Mei, Y., and Zhang, L.: Copula-based bivariate flood frequency analysis in a changing climate—  
10 A case study in the Huai River Basin, China, *Journal of Earth Science*, 27, 37-46, 2016a.

11 Duan, K., Sun, G., Sun, S., Caldwell, P. V., Cohen, E., McNulty, S. G., Aldridge, H. D., and Zhang, Y.:  
12 Divergence of ecosystem services in U.S. National Forests and Grasslands under a changing climate,  
13 *Scientific Reports*, 10.1038/srep24441, 2016b.

14 Duan, K., Sun, G., Zhang, Y., Yahya, K., Wang, K., Madden, J. M., Caldwell, P. V., Cohen, E. C., and McNulty,  
15 S. G.: Impact of air pollution induced climate change on water availability and ecosystem productivity in  
16 the conterminous United States, *Climatic Change*, 140, 259-272, 10.1007/s10584-016-1850-7, 2017.

17 Feng, S., and Fu, Q.: Expansion of global drylands under a warming climate, *Atmos. Chem. Phys*, 13,  
18 10,081-010,094, 2013.

19 Ficklin, D. L., Luo, Y., Luedeling, E., and Zhang, M.: Climate change sensitivity assessment of a highly  
20 agricultural watershed using SWAT, *Journal of Hydrology*, 374, 16-29, 2009.

21 Gedney, N., Cox, P., Betts, R., Boucher, O., Huntingford, C., and Stott, P.: Detection of a direct carbon  
22 dioxide effect in continental river runoff records, *Nature*, 439, 835-838, 2006.

23 Gibbons, J. D., and Chakraborti, S.: *Nonparametric statistical inference*, Springer, Berlin Heidelberg, 2011.

24 Giuntoli, I., Vidal, J.-P., Prudhomme, C., and Hannah, D. M.: Future hydrological extremes: the  
25 uncertainty from multiple global climate and global hydrological models, *Earth System Dynamics*, 6,  
26 267-285, 2015.

27 Grant, G. E., Tague, C. L., and Allen, C. D.: Watering the forest for the trees: an emerging priority for  
28 managing water in forest landscapes, *Frontiers in Ecology and the Environment*, 11, 314-321, 2013.

29 Gupta, S. C., Kessler, A. C., Brown, M. K., and Zvomuya, F.: Climate and agricultural land use change  
30 impacts on streamflow in the upper midwestern United States, *Water Resources Research*, 51, 5301-  
31 5317, 2015.

32 IPCC: *Climate Change 2014: Synthesis Report. Contribution of Working Groups I, II and III to the Fifth*  
33 *Assessment Report of the Intergovernmental Panel on Climate Change*, IPCC, Geneva,  
34 Switzerland9291691437, 2014.

35 Jackson, R. B., Jobbágy, E. G., Avissar, R., Roy, S. B., Barrett, D. J., Cook, C. W., Farley, K. A., Le Maitre, D.  
36 C., McCarl, B. A., and Murray, B. C.: Trading water for carbon with biological carbon sequestration,  
37 *Science*, 310, 1944-1947, 2005.

38 Jung, I.-W., Moradkhani, H., and Chang, H.: Uncertainty assessment of climate change impacts for  
39 hydrologically distinct river basins, *Journal of Hydrology*, 466, 73-87, 2012.

40 Karl, T. R., and Riebsame, W. E.: The impact of decadal fluctuations in mean precipitation and  
41 temperature on runoff: a sensitivity study over the United States, *Climatic Change*, 15, 423-447, 1989.

42 Kay, A., Davies, H., Bell, V., and Jones, R.: Comparison of uncertainty sources for climate change impacts:  
43 flood frequency in England, *Climatic Change*, 92, 41-63, 2009.

44 Kingston, D. G., Todd, M. C., Taylor, R. G., Thompson, J. R., and Arnell, N. W.: Uncertainty in the

1 estimation of potential evapotranspiration under climate change, *Geophysical Research Letters*, 36,  
2 L20403, 10.1029/2009GL040267, 2009.

3 Koren, V., Smith, M., and Duan, Q.: Use of a priori parameter estimates in the derivation of spatially  
4 consistent parameter sets of rainfall - runoff models, *Calibration of Watershed Models*, 6, AGU,  
5 Washington, D.C., 239-254 pp., 2003.

6 Livneh, B., Rosenberg, E. A., Lin, C., Nijssen, B., Mishra, V., Andreadis, K. M., Maurer, E. P., and  
7 Lettenmaier, D. P.: A long-term hydrologically based dataset of land surface fluxes and states for the  
8 conterminous United States: update and extensions, *Journal of Climate*, 26, 9384-9392, 2013.

9 Lu, J., Sun, G., McNulty, S. G., and Amatya, D. M.: A comparison of six potential evapotranspiration  
10 methods for regional use in the southeastern United States, *Journal of American Water Resources*  
11 *Association*, 41, 621-633, 2005.

12 Lutz, A., Immerzeel, W., Shrestha, A., and Bierkens, M.: Consistent increase in High Asia's runoff due to  
13 increasing glacier melt and precipitation, *Nature Climate Change*, 4, 587-592, 2014.

14 Mauget, S. A.: Multidecadal regime shifts in US streamflow, precipitation, and temperature at the end  
15 of the twentieth century, *Journal of Climate*, 16, 3905-3916, 2003.

16 McCabe, G. J., and Wolock, D. M.: A step increase in streamflow in the conterminous United States,  
17 *Geophysical Research Letters*, 29, 2002.

18 McCabe, G. J., and Markstrom, S. L.: A monthly water-balance model driven by a graphical user interface,  
19 *Geological Survey (US)2331-1258*, 2007.

20 McCabe, G. J., and Wolock, D. M.: Independent effects of temperature and precipitation on modeled  
21 runoff in the conterminous United States, *Water Resources Research*, 47, 10.1029/2011WR010630,  
22 2011.

23 McCabe, G. J., and Wolock, D. M.: Variability and Trends in Runoff Efficiency in the Conterminous United  
24 States, *Journal of the American Water Resources Association*, 10.1111/1752-1688.12431, 2016.

25 McVicar, T. R., Roderick, M. L., Donohue, R. J., Li, L. T., Van Niel, T. G., Thomas, A., Grieser, J., Jhajharia,  
26 D., Himri, Y., and Mahowald, N. M.: Global review and synthesis of trends in observed terrestrial near-  
27 surface wind speeds: Implications for evaporation, *Journal of Hydrology*, 416, 182-205, 2012.

28 Mearns, L. O., Arritt, R., Biner, S., Bukovsky, M. S., McGinnis, S., Sain, S., Caya, D., Correia Jr, J., Flory, D.,  
29 and Gutowski, W.: The North American regional climate change assessment program: overview of phase  
30 I results, *Bulletin of the American Meteorological Society*, 93, 1337-1362, 2012.

31 Milly, P. C., Dunne, K. A., and Vecchia, A. V.: Global pattern of trends in streamflow and water availability  
32 in a changing climate, *Nature*, 438, 347-350, 2005.

33 Milly, P. C., Betancourt, J., Falkenmark, M., Hirsch, R. M., Kundzewicz, Z. W., Lettenmaier, D. P., and  
34 Stouffer, R. J.: Stationarity is dead: Whither water management?, *Science*, 319, 573-574, 2008.

35 Milly, P. C., and Dunne, K. A.: On the hydrologic adjustment of climate-model projections: The potential  
36 pitfall of potential evapotranspiration, *Earth Interactions*, 15, 1-14, 2011.

37 Moss, R. H., Edmonds, J. A., Hibbard, K. A., Manning, M. R., Rose, S. K., Van Vuuren, D. P., Carter, T. R.,  
38 Emori, S., Kainuma, M., and Kram, T.: The next generation of scenarios for climate change research and  
39 assessment, *Nature*, 463, 747-756, 2010.

40 Nash, L. L., and Gleick, P. H.: Sensitivity of streamflow in the Colorado basin to climatic changes, *Journal*  
41 *of hydrology*, 125, 221-241, 1991.

42 Piao, S., Ciais, P., Huang, Y., Shen, Z., Peng, S., Li, J., Zhou, L., Liu, H., Ma, Y., and Ding, Y.: The impacts of  
43 climate change on water resources and agriculture in China, *Nature*, 467, 43-51, 2010.

44 Ryberg, K. R., Lin, W., and Vecchia, A. V.: Impact of climate variability on runoff in the North-Central



1 United States, *Journal of Hydrologic Engineering*, 19, 148-158, 2014.

2 Schewe, J., Heinke, J., Gerten, D., Haddeland, I., Arnell, N. W., Clark, D. B., Dankers, R., Eisner, S., Fekete,  
3 B. M., and Colón-González, F. J.: Multimodel assessment of water scarcity under climate change,  
4 *Proceedings of the National Academy of Sciences*, 111, 3245-3250, 2014.

5 Seager, R., Ting, M., Li, C., Naik, N., Cook, B., Nakamura, J., and Liu, H.: Projections of declining surface-  
6 water availability for the southwestern United States, *Nature Climate Change*, 3, 482-486, 2013.

7 Sheffield, J., Wood, E. F., and Roderick, M. L.: Little change in global drought over the past 60 years,  
8 *Nature*, 491, 435-438, 2012.

9 Sospedra - Alfonso, R., Melton, J. R., and Merryfield, W. J.: Effects of temperature and precipitation on  
10 snowpack variability in the Central Rocky Mountains as a function of elevation, *Geophysical Research*  
11 *Letters*, 42, 4429-4438, 2015.

12 Sun, G., Alstad, K., Chen, J., Chen, S., Ford, C. R., Lin, G., Liu, C., Lu, N., McNulty, S. G., and Miao, H.: A  
13 general predictive model for estimating monthly ecosystem evapotranspiration, *Ecohydrology*, 4, 245-  
14 255, 2011a.

15 Sun, G., Caldwell, P., Noormets, A., McNulty, S. G., Cohen, E., Moore Myers, J., Domec, J. C., Treasure, E.,  
16 Mu, Q., and Xiao, J.: Upscaling key ecosystem functions across the conterminous United States by a  
17 water - centric ecosystem model, *Journal of Geophysical Research*, 116, 10.1029/2010JG001573,  
18 2011b.

19 Sun, G., Caldwell, P. V., and McNulty, S. G.: Modelling the potential role of forest thinning in maintaining  
20 water supplies under a changing climate across the conterminous United States, *Hydrological Processes*,  
21 29, 5016-5030, 2015a.

22 Sun, S., Sun, G., Caldwell, P., McNulty, S., Cohen, E., Xiao, J., and Zhang, Y.: Drought impacts on ecosystem  
23 functions of the US National Forests and Grasslands: Part I evaluation of a water and carbon balance  
24 model, *Forest Ecology and Management*, 353, 260-268, 2015b.

25 Teixeira, E. I., Fischer, G., van Velthuisen, H., Walter, C., and Ewert, F.: Global hot-spots of heat stress on  
26 agricultural crops due to climate change, *Agricultural and Forest Meteorology*, 170, 206-215, 2013.

27 Trenberth, K. E., Dai, A., van der Schrier, G., Jones, P. D., Barichivich, J., Briffa, K. R., and Sheffield, J.:  
28 Global warming and changes in drought, *Nature Climate Change*, 4, 17-22, 2014.

29 Vano, J. A., Das, T., and Lettenmaier, D. P.: Hydrologic sensitivities of Colorado River runoff to changes in  
30 precipitation and temperature\*, *Journal of Hydrometeorology*, 13, 932-949, 2012.

31 Vörösmarty, C. J., Federer, C. A., and Schloss, A. L.: Potential evaporation functions compared on US  
32 watersheds: Possible implications for global-scale water balance and terrestrial ecosystem modeling,  
33 *Journal of Hydrology*, 207, 147-169, 1998.

34 Vörösmarty, C. J., Green, P., Salisbury, J., and Lammers, R. B.: Global water resources: vulnerability from  
35 climate change and population growth, *science*, 289, 284-288, 2000.

36 Vose, J. M., Miniati, C. F., Luce, C. H., Asbjornsen, H., Caldwell, P. V., Campbell, J. L., Grant, G. E., Isaak, D.  
37 J., Loheide, S. P., and Sun, G.: Ecohydrological implications of drought for forests in the United States,  
38 *Forest Ecology and Management*, 10.1016/j.foreco.2016.03.025, 2016.

39 Wilby, R. L., and Harris, I.: A framework for assessing uncertainties in climate change impacts: Low -  
40 flow scenarios for the River Thames, UK, *Water Resources Research*, 42, 2006.

41 Woodhouse, C. A., Pederson, G. T., Morino, K., McAfee, S. A., and McCabe, G. J.: Increasing influence of  
42 air temperature on upper Colorado River streamflow, *Geophysical Research Letters*, 43, 2174-2181,  
43 2016.

44 Zhang, D., Cong, Z., Ni, G., Yang, D., and Hu, S.: Effects of snow ratio on annual runoff within the Budyko

1 framework, *Hydrology and Earth System Sciences*, 19, 1977-1992, 2015.  
2 Zhang, L., Dawes, W., and Walker, G.: Response of mean annual evapotranspiration to vegetation  
3 changes at catchment scale, *Water resources research*, 37, 701-708, 2001.  
4 Zhou, G., Wei, X., Chen, X., Zhou, P., Liu, X., Xiao, Y., Sun, G., Scott, D. F., Zhou, S., and Han, L.: Global  
5 pattern for the effect of climate and land cover on water yield, *Nature communications*, 6,  
6 10.1038/ncomms6918, 2015.  
7

1 *Acknowledgements.* This work was supported by the National Science Foundation  
2 EaSM program (AGS-1049200) awarded to North Carolina State University, and the  
3 Eastern Forest Environmental Threat Assessment Center (EFETAC), USDA Forest  
4 Service, Raleigh, NC. The MACAv2-LIVNEH dataset was produced under the  
5 Northwest Climate Science Center (NW CSC) US Geological Survey Grant Number  
6 G12AC20495. Partial support was provided by the Natural Science Foundation of  
7 Jiangsu Province, China (BK20151525); the Pine Integrated Network: Education,  
8 Mitigation, and Adaptation project (PINEMAP), which is a Coordinated Agricultural  
9 Project funded by the USDA National Institute of Food and Agriculture, Award #2011-  
10 68002-30185. The authors would like to give special thanks to Drs. Dennis Lettenmaier,  
11 Paul CD Milly, William Farmer, Brian Finlayson, and two anonymous reviewers for  
12 their valuable comments and suggestions.

13 *Author contributions.* K.D. and G.S. designed the study. K.D. performed the analysis.  
14 E.C., H.A., S.S., D.C., and X.Z. helped collect the data. All authors contributed to the  
15 interpretation of the results. K.D. wrote the initial draft, and G.S., P.C., S.M., and Y.Z.  
16 refined the manuscript.

17 *Competing interests.* The authors declare that they have no conflict of interest.

18

19

# 1 Tables

2 **Table 1.** List of the 20 climate models and the changes in mean annual precipitation and temperature  
 3 over the conterminous United States (CONUS) from the baseline scenario (B) to future scenarios S1  
 4 (RCP4.5/2030s), S2 (RCP4.5/2080s), S3 (RCP8.5/2030s), and S4 (RCP8.5/2080s).

| GCM            | Country   | Precipitation (mm yr <sup>-1</sup> ) |     |     |     |     | Temperature (°C) |      |      |      |      |
|----------------|-----------|--------------------------------------|-----|-----|-----|-----|------------------|------|------|------|------|
|                |           | B                                    | S1  | S2  | S3  | S4  | B                | S1   | S2   | S3   | S4   |
| bcc-csm1-1     | China     | 787                                  | -3  | +13 | +33 | -5  | 11.4             | +1.7 | +2.4 | +1.9 | +4.8 |
| bcc-csm1-1-m   | China     | 786                                  | +18 | -18 | +29 | +33 | 11.4             | +1.5 | +2.4 | +1.7 | +4.3 |
| BNU-ESM        | China     | 798                                  | +51 | +42 | +25 | +45 | 11.5             | +1.9 | +3.2 | +2.0 | +5.4 |
| CanESM2        | Canada    | 800                                  | +14 | +42 | +19 | +83 | 11.3             | +2.3 | +3.5 | +2.4 | +5.8 |
| CCSM4          | USA       | 783                                  | +29 | +29 | +18 | +58 | 11.5             | +1.5 | +2.5 | +1.9 | +4.6 |
| CNRM-CM5       | France    | 780                                  | +46 | +56 | +40 | +85 | 11.4             | +1.4 | +2.8 | +1.6 | +4.6 |
| CSIRO-Mk3-6-0  | Australia | 780                                  | +14 | +84 | +24 | +74 | 11.2             | +2.0 | +3.4 | +2.0 | +5.6 |
| GFDL-ESM2M     | USA       | 787                                  | +6  | +20 | +32 | +31 | 11.3             | +1.6 | +2.2 | +1.7 | +4.2 |
| GFDL-ESM2G     | USA       | 791                                  | +21 | +36 | +38 | +12 | 11.4             | +1.2 | +1.7 | +1.2 | +3.7 |
| HadGEM2-ES     | UK        | 784                                  | +16 | +7  | +18 | +7  | 11.3             | +2.2 | +3.8 | +2.5 | +6.8 |
| HadGEM2-CC     | UK        | 779                                  | +23 | +39 | +5  | +32 | 11.3             | +2.3 | +4.2 | +2.7 | +6.7 |
| inmcm4         | Russia    | 779                                  | -7  | +4  | +0  | +13 | 11.4             | +0.9 | +1.7 | +1.1 | +3.4 |
| IPSL-CM5A-LR   | France    | 780                                  | +8  | +14 | +13 | -8  | 11.5             | +1.8 | +3.0 | +1.8 | +5.8 |
| IPSL-CM5A-MR   | France    | 789                                  | -4  | +13 | -25 | -70 | 11.3             | +1.9 | +3.2 | +2.3 | +6.0 |
| IPSL-CM5B-LR   | France    | 781                                  | +23 | +62 | +34 | +82 | 11.4             | +1.5 | +2.4 | +1.7 | +4.4 |
| MIROC5         | Japan     | 788                                  | +9  | +10 | +24 | +6  | 11.2             | +2.3 | +3.6 | +2.4 | +5.7 |
| MIROC-ESM      | Japan     | 791                                  | +56 | +37 | +30 | +9  | 11.3             | +2.1 | +4.1 | +2.6 | +6.6 |
| MIROC-ESM-CHEM | Japan     | 784                                  | +12 | +38 | +26 | +10 | 11.4             | +2.4 | +4.0 | +2.7 | +6.9 |
| MRI-CGCM3      | Japan     | 783                                  | +20 | +47 | +38 | +87 | 11.4             | +0.8 | +1.7 | +1.0 | +3.2 |
| NorESM1-M      | Norway    | 784                                  | +13 | +31 | +25 | +63 | 11.3             | +1.8 | +3.1 | +2.2 | +5.1 |

5

1 **Table 2.** Comparison of multi-model averaged contributions (%) of precipitation (*P*) and temperature (*T*) to changes in runoff in the 18 Water Resource Regions (WRRs) and  
 2 entire CONUS in historical period (1961-2010) and future scenarios S1 (RCP4.5/2030s), S2 (RCP4.5/2080s), S3 (RCP8.5/2030s), and S4 (RCP8.5/2080s). The larger  
 3 contributor identified by multi-model ensemble means is bolded, and the significant larger contributor identified by Wilcoxon signed-rank test (at 5 % significance) is underlined.

| WRR | Historical |           | Projections based on PM PET |           |           |           |           |           |           |           | Projections based on Hamon PET |           |           |           |           |           |           |           |
|-----|------------|-----------|-----------------------------|-----------|-----------|-----------|-----------|-----------|-----------|-----------|--------------------------------|-----------|-----------|-----------|-----------|-----------|-----------|-----------|
|     |            |           | S1                          |           | S2        |           | S3        |           | S4        |           | S1                             |           | S2        |           | S3        |           | S4        |           |
|     | <i>P</i>   | <i>T</i>  | <i>P</i>                    | <i>T</i>  | <i>P</i>  | <i>T</i>  | <i>P</i>  | <i>T</i>  | <i>P</i>  | <i>T</i>  | <i>P</i>                       | <i>T</i>  | <i>P</i>  | <i>T</i>  | <i>P</i>  | <i>T</i>  | <i>P</i>  | <i>T</i>  |
| 1   | <b>88</b>  | 9         | 36                          | <b>36</b> | 36        | <b>38</b> | 34        | <b>38</b> | 31        | <u>42</u> | <u>61</u>                      | 38        | <b>58</b> | 40        | <u>57</u> | 41        | <b>53</b> | 46        |
| 2   | <b>80</b>  | 17        | 27                          | <b>40</b> | 28        | <u>41</u> | 30        | <b>39</b> | 28        | <u>43</u> | 47                             | <b>50</b> | 49        | <b>50</b> | <b>51</b> | 47        | 46        | <b>52</b> |
| 3   | <b>60</b>  | 30        | 31                          | <b>37</b> | 26        | <u>41</u> | 30        | <b>38</b> | 24        | <u>44</u> | 43                             | <b>49</b> | 38        | <u>56</u> | 41        | <b>52</b> | 32        | <u>60</u> |
| 4   | <b>83</b>  | 13        | 24                          | <u>44</u> | 23        | <u>46</u> | 29        | <u>41</u> | 23        | <u>47</u> | 44                             | <b>54</b> | 42        | <u>57</u> | <b>50</b> | 48        | 40        | <u>58</u> |
| 5   | <b>73</b>  | 22        | 23                          | <u>42</u> | 23        | <u>44</u> | 29        | <b>40</b> | 25        | <u>46</u> | 40                             | <b>57</b> | 38        | <u>59</u> | 46        | <b>51</b> | 37        | <u>60</u> |
| 6   | <b>64</b>  | 30        | 28                          | <b>40</b> | 27        | <u>42</u> | 32        | <b>38</b> | 26        | <u>45</u> | 41                             | <b>54</b> | 40        | <u>56</u> | 46        | <b>49</b> | 37        | <u>58</u> |
| 7   | <b>89</b>  | 6         | 23                          | <u>47</u> | 19        | <u>51</u> | 23        | <u>48</u> | 20        | <u>52</u> | 40                             | <u>57</u> | 32        | <u>65</u> | 37        | <u>59</u> | 32        | <u>65</u> |
| 8   | <b>48</b>  | 37        | 27                          | <b>39</b> | 23        | <u>43</u> | 24        | <u>42</u> | 24        | <u>46</u> | 38                             | <b>53</b> | 34        | <u>58</u> | 35        | <u>56</u> | 29        | <u>61</u> |
| 9   | <b>89</b>  | 8         | 22                          | <u>47</u> | 20        | <u>49</u> | 26        | <u>45</u> | 20        | <u>43</u> | 37                             | <b>56</b> | 34        | <u>61</u> | 40        | <b>53</b> | 33        | <u>57</u> |
| 10  | <b>81</b>  | 6         | 19                          | <u>47</u> | 18        | <u>50</u> | 18        | <u>49</u> | 20        | <u>46</u> | 35                             | <u>57</u> | 32        | <u>62</u> | 32        | <u>60</u> | 33        | <u>59</u> |
| 11  | <b>88</b>  | 4         | 20                          | <u>42</u> | 19        | <u>45</u> | 18        | <u>44</u> | 18        | <u>47</u> | 30                             | <u>55</u> | 29        | <u>60</u> | 27        | <u>58</u> | 26        | <u>63</u> |
| 12  | <b>74</b>  | 14        | <b>35</b>                   | 29        | 27        | <b>35</b> | 30        | <b>32</b> | 27        | <u>39</u> | <b>44</b>                      | 38        | 37        | <b>46</b> | 38        | <b>42</b> | 31        | <u>51</u> |
| 13  | <b>71</b>  | 18        | 25                          | <u>36</u> | 27        | <b>38</b> | 26        | <u>35</u> | 22        | <u>42</u> | 35                             | <u>53</u> | 36        | <u>56</u> | 37        | <b>53</b> | 28        | <u>61</u> |
| 14  | 30         | <b>51</b> | 21                          | <u>48</u> | 25        | <u>48</u> | 20        | <u>49</u> | 24        | <u>49</u> | 31                             | <u>64</u> | 36        | <u>60</u> | 32        | <u>64</u> | 31        | <u>61</u> |
| 15  | <b>72</b>  | 17        | 28                          | <b>33</b> | <b>36</b> | 32        | <b>33</b> | 32        | <b>36</b> | 29        | 35                             | <b>52</b> | 41        | <b>48</b> | 43        | <b>47</b> | 37        | <b>49</b> |
| 16  | <b>65</b>  | 23        | 21                          | <u>45</u> | 24        | <u>46</u> | 23        | <u>45</u> | 29        | <u>43</u> | 34                             | <u>59</u> | 36        | <u>58</u> | 32        | <u>60</u> | 38        | <b>51</b> |
| 17  | <b>91</b>  | 7         | 28                          | <b>42</b> | 28        | <u>43</u> | 29        | <u>42</u> | 31        | <u>42</u> | 44                             | <b>54</b> | 44        | <b>54</b> | 45        | <b>53</b> | 47        | <b>51</b> |
| 18  | <b>95</b>  | 4         | <u>47</u>                   | 29        | <b>43</b> | 32        | <u>46</u> | 30        | <b>46</b> | 30        | <u>58</u>                      | 36        | <b>54</b> | 41        | <b>56</b> | 39        | <b>54</b> | 42        |

1

---

|       |    |    |  |    |           |    |           |    |           |    |           |  |    |           |    |           |    |           |    |           |
|-------|----|----|--|----|-----------|----|-----------|----|-----------|----|-----------|--|----|-----------|----|-----------|----|-----------|----|-----------|
| CONUS | 57 | 29 |  | 20 | <u>45</u> | 20 | <u>47</u> | 24 | <u>43</u> | 21 | <u>50</u> |  | 35 | <u>58</u> | 35 | <u>60</u> | 40 | <u>55</u> | 33 | <u>62</u> |
|-------|----|----|--|----|-----------|----|-----------|----|-----------|----|-----------|--|----|-----------|----|-----------|----|-----------|----|-----------|

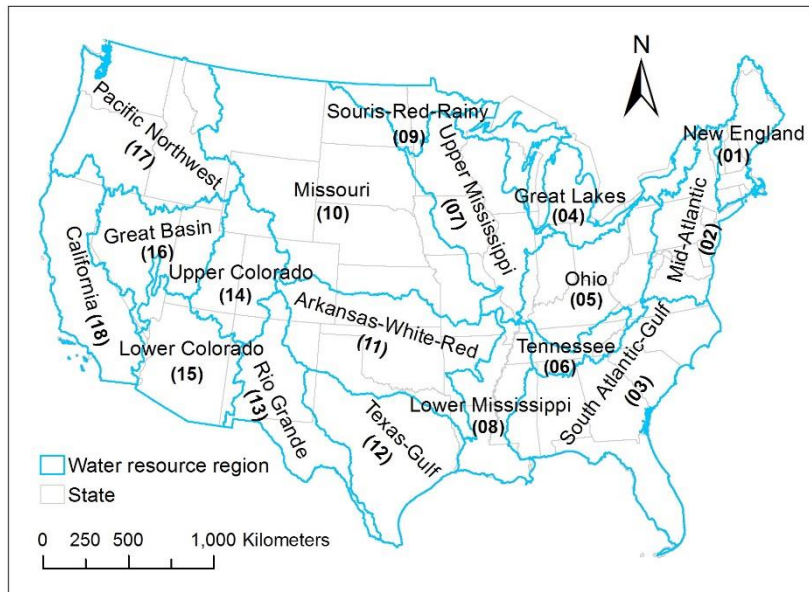
1 **Table 3.** Cross comparison of the areal proportions (%) with different dominant driving factors and  
 2 changing directions of runoff (*R*) in the future scenarios S1 (RCP4.5/2030s), S2 (RCP4.5/2080s), S3  
 3 (RCP8.5/2030s), and S4 (RCP8.5/2080s). The areas where a variable is the largest driving factor  
 4 identified by multi-model ensemble means is marked in the brackets. The areas where a variable is  
 5 identified as the ‘dominant’ factor are bolded. A climate variable is identified as the ‘dominant’ one only  
 6 when 80 % or more of the 20 GCMs agree that it is the largest driving factor of runoff change.

| Scenario                 | S1               | S2             | S3               | S4             |
|--------------------------|------------------|----------------|------------------|----------------|
| <i>Precipitation</i>     |                  |                |                  |                |
| <i>R</i> ↗ <sup>a</sup>  | <b>4</b> (10)    | <b>7</b> (17)  | <b>6</b> (15)    | <b>6</b> (21)  |
| <i>R</i> ↘               | <b>0.2</b> (0.2) | 0              | <b>0.2</b> (0.2) | 0 (0.7)        |
| <i>Temperature</i>       |                  |                |                  |                |
| <i>R</i> ↗               | <b>9</b> (51)    | <b>15</b> (45) | <b>7</b> (55)    | <b>13</b> (26) |
| <i>R</i> ↘               | <b>15</b> (38)   | <b>23</b> (37) | <b>14</b> (30)   | <b>28</b> (42) |
| <i>Specific humidity</i> |                  |                |                  |                |
| <i>R</i> ↗               | 0 (0.2)          | 0 (2)          | 0 (0.2)          | <b>0.8</b> (5) |
| <i>R</i> ↘               | 0 (0.2)          | 0 (0.4)        | 0                | <b>1</b> (5)   |

7 <sup>a</sup> “↗” and “↘” indicate increase and decrease in the multi-model means of runoff, respectively.

8

1 **Figures**



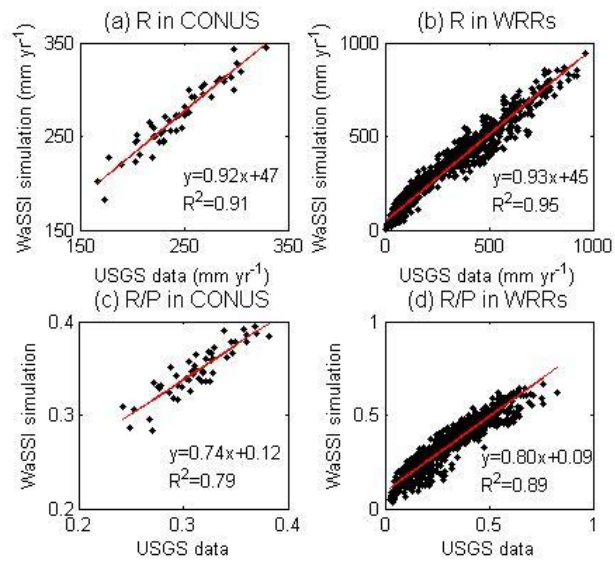
2

3 **Figure 1.** Location of the 18 Water Resource Regions (WRRs) in the conterminous United States  
4 (CONUS).

5



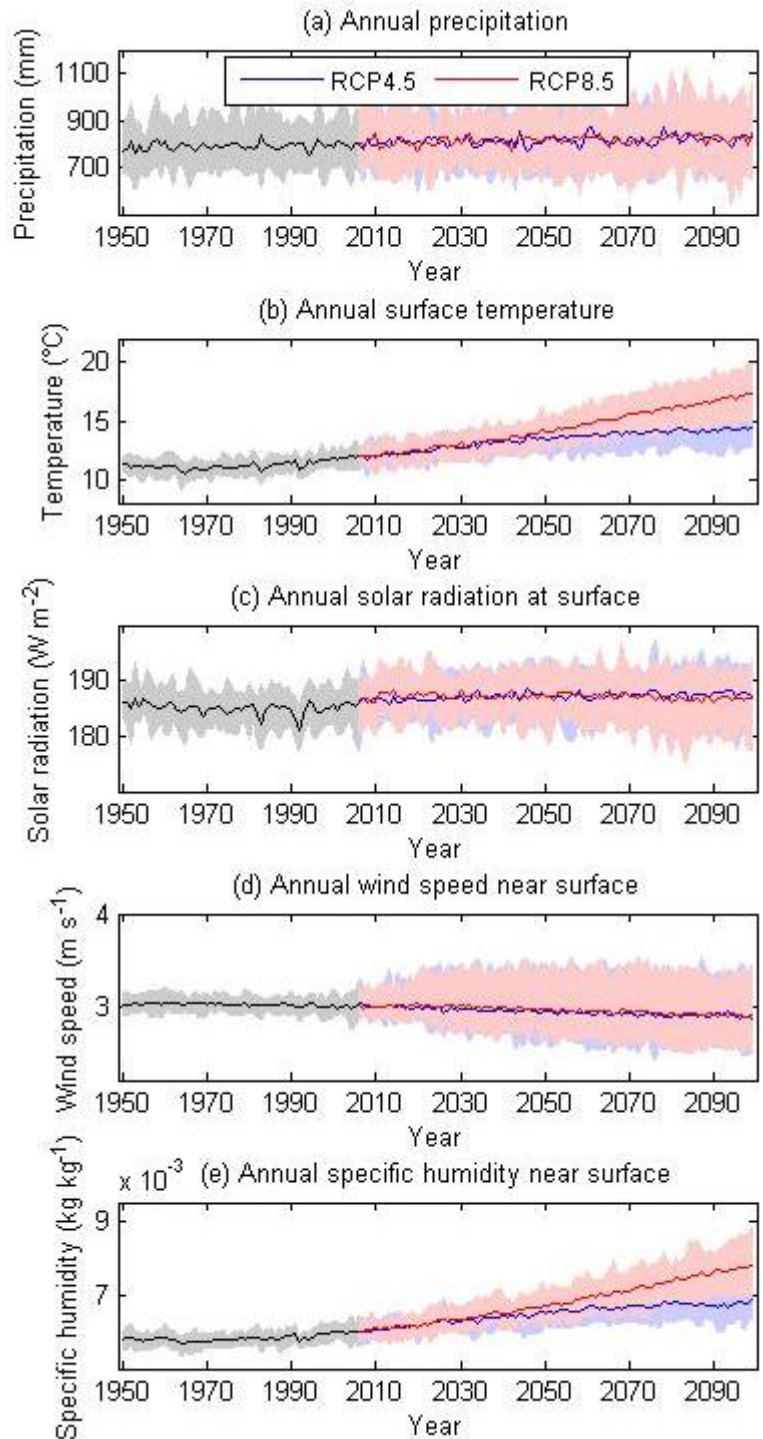
1



2

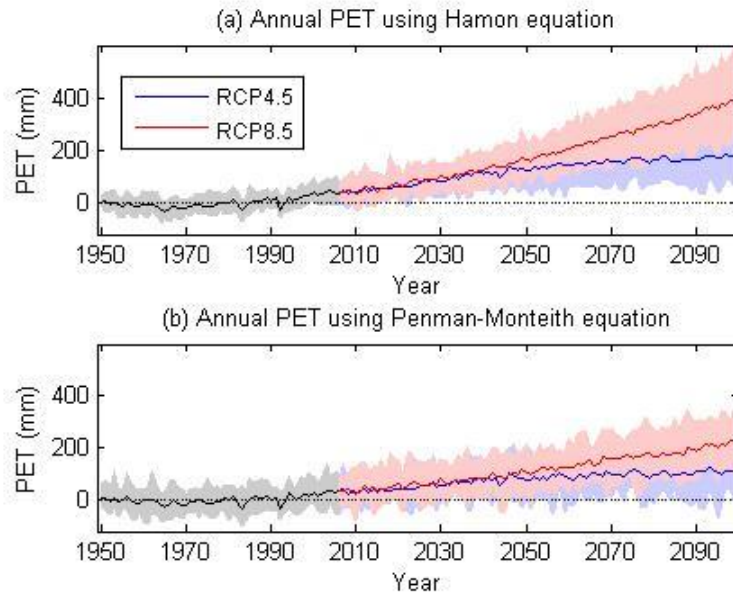
3 **Figure 2.** Validations of the WaSSI model at the conterminous United States (CONUS) and Water  
4 Resource Region (WRR) levels. **a-b**, Comparisons of simulated annual runoff ( $R$ ) (mm yr<sup>-1</sup>) against  
5 USGS observed data in 1961-2010 over the entire CONUS (**a**) and in 18 WRRs (**b**). **c-d**, Comparisons  
6 of simulated runoff coefficient (runoff/precipitation, R/P) against that derived from USGS observed data  
7 in the CONUS (**c**) and WRRs (**d**).

8



1  
 2 **Figure 3.** Temporal variations of annual mean precipitation (a), surface air temperature (b), solar  
 3 radiation at surface (c), wind speed near surface (d), and specific humidity near surface (e) over the  
 4 CONUS. Thick lines and the shading denote the multi-model ensemble means and uncertainty ranges of  
 5 the 20 GCMs, respectively.

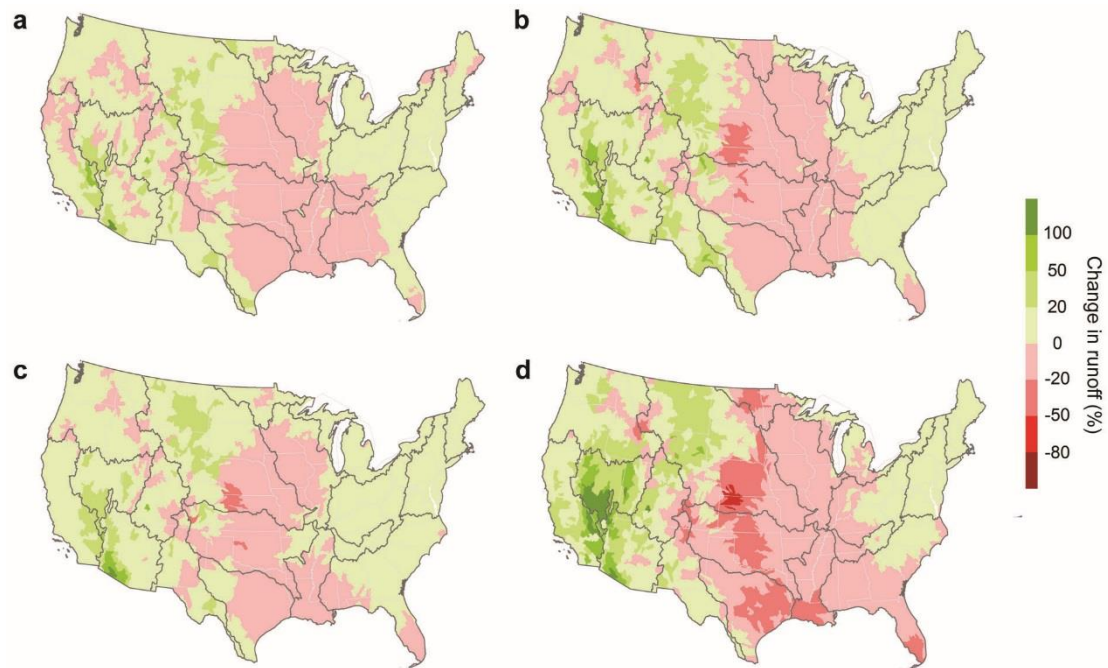
6



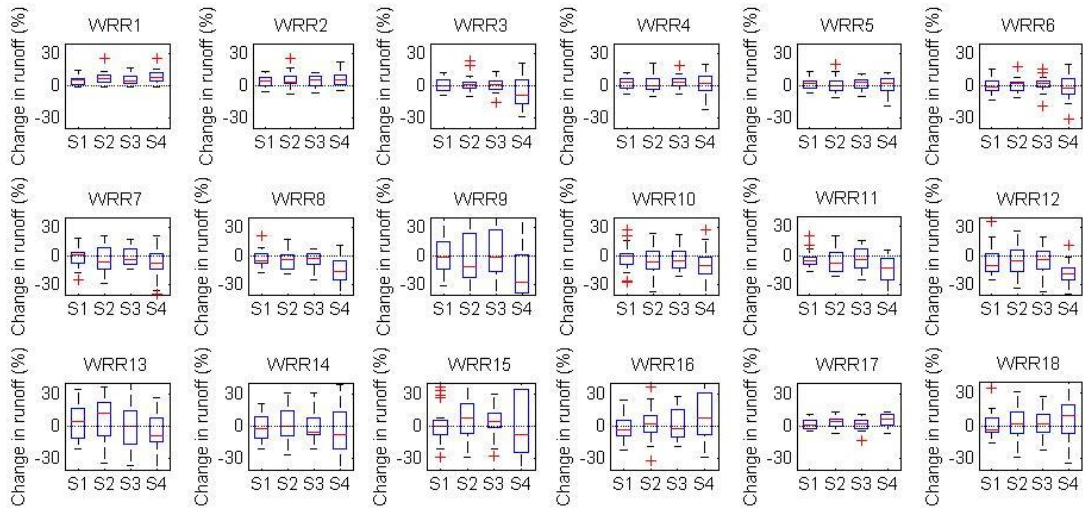
1

2 **Figure 4.** Temporal variations of changes in annual potential evapotranspiration (PET) over the CONUS  
 3 against the baseline level (1970-1999). Thick lines and the shading denote the ensemble means and  
 4 uncertainty ranges of the 20 GCMs, respectively.

5



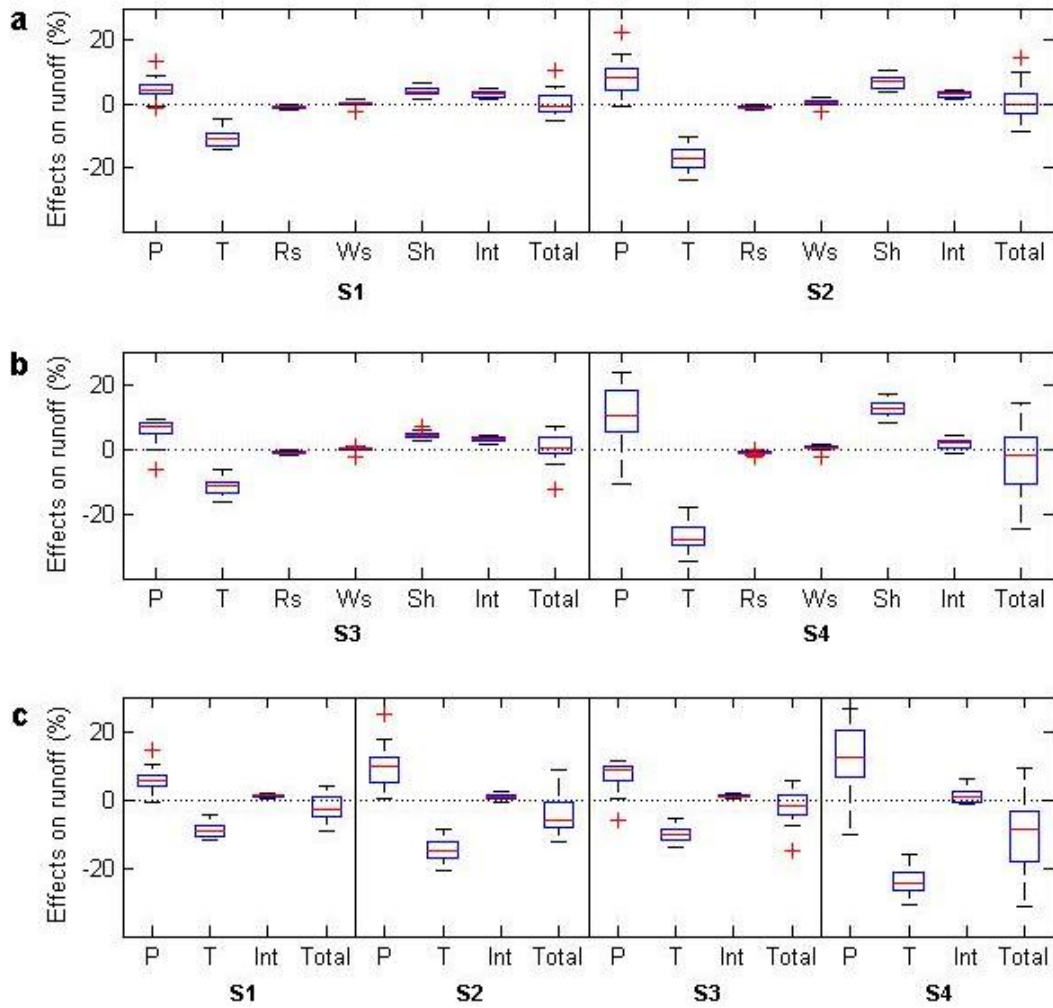
1  
 2 **Figure 5.** Projected changes in multi-year mean annual runoff (%) at HUC-8 watershed scale. **a-d,**  
 3 Changes from the baseline to S1 (RCP4.5/2030s) (**a**), S2 (RCP4.5/2080s) (**b**), S3 (RCP8.5/2030s) (**c**),  
 4 and S4 (RCP8.5/2080s) (**d**) scenarios. The maps display the multi-model mean changes from the 20  
 5 GCMs.  
 6



1

2 **Figure 6.** Area-averaged changes in runoff in the 18 Water Resource Regions (WRRs) in the future  
 3 scenarios. The four future scenarios are denoted by S1 (RCP4.5/2030s), S2 (RCP4.5/2080s), S3  
 4 (RCP8.5/2030s), and S4 (RCP8.5/2080s) in the x-axis. The vertical spread of the box-whisker plots  
 5 shows the different results projected from the 20 GCMs, with the boxes covering the ranges from 25 %  
 6 quartile to 75 % quartile of the distributions (Inter-Quartile Range, IQR) and the red lines within each  
 7 box marking the median values. Points outside the whiskers are taken as extreme outliers and marked by  
 8 plus signs.

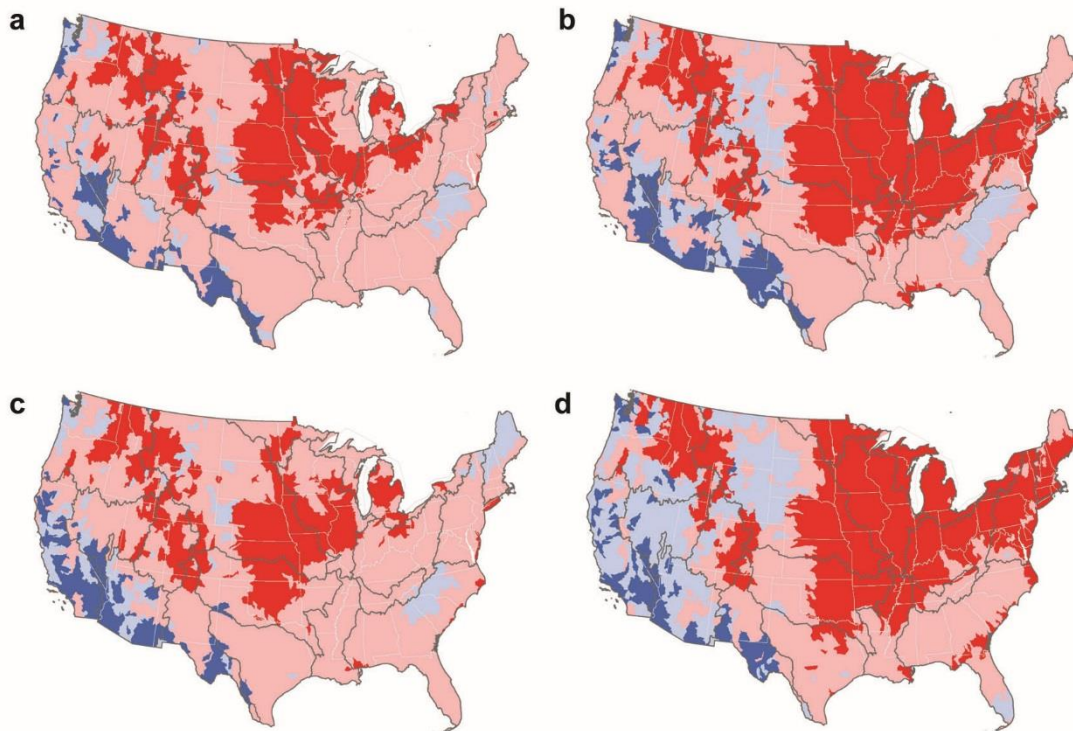
9



1  
2  
3  
4  
5  
6  
7  
8  
9  
10  
11

**Figure 7.** Independent effects of the climate variables over the conterminous United States (CONUS) in the future scenarios S1 (RCP4.5/2030s), S2 (RCP4.5/2080s), S3 (RCP8.5/2030s), and S4 (RCP8.5/2080s). **a-b,** Effects of precipitation (*P*), temperature (*T*), solar radiation (*Rs*), wind speed (*Ws*), specific humidity (*Sh*), interactions among the variables (*Int*), and their sum (*Total*) on runoff based on the projections of Penman-Monteith PET. **c,** Effects of precipitation (*P*), temperature (*T*), interaction between *P* and *T* (*Int*), and their sum (*Total*) on runoff based on the projections of Hamon PET. The format of the box-whisker plots is the same as that in Fig. 6.





1

2 **Figure 8.** Relative importance of  $P$  and  $T$  in affecting runoff change across the HUC-8 watersheds in the  
 3 future scenarios of S1 (RCP4.5/2030s) (a), S2 (RCP4.5/2080s) (b), S3 (RCP8.5/2030s) (c), and S4  
 4 (RCP8.5/2080s) (d). The watersheds under larger influence of  $P$  and  $T$  are marked with blue and red  
 5 colors, respectively. The dark colors denote the areas where 80 % or more of the 20 GCMs agree on the  
 6 sign, while the light colors denote the results of ensemble average.

7